

Calvin University

Calvin Digital Commons

University Faculty Publications and Creative Works

University Faculty Scholarship

2-5-2007

Recollision dynamics and time delay in strong-field double ionization

Stanley L. Haan
Calvin University

L. Breen
Calvin University

A. Karim
Calvin University

Joseph H. Eberly
University of Rochester

Follow this and additional works at: https://digitalcommons.calvin.edu/calvin_facultypubs



Part of the [Optics Commons](#)

Recommended Citation

Haan, Stanley L.; Breen, L.; Karim, A.; and Eberly, Joseph H., "Recollision dynamics and time delay in strong-field double ionization" (2007). *University Faculty Publications and Creative Works*. 487.
https://digitalcommons.calvin.edu/calvin_facultypubs/487

This Article is brought to you for free and open access by the University Faculty Scholarship at Calvin Digital Commons. It has been accepted for inclusion in University Faculty Publications and Creative Works by an authorized administrator of Calvin Digital Commons. For more information, please contact digitalcommons@calvin.edu.

Recollision Dynamics and Time Delay in Strong-Field Double Ionization

S.L. Haan, L. Breen, A. Karim

*Department of Physics and Astronomy, Calvin College,
Grand Rapids MI 49546 USA*

haan@calvin.edu

<http://www.calvin.edu/haan>

J.H. Eberly

*Department of Physics and Astronomy, University of Rochester,
Rochester, NY 14627 USA*

eberly@pas.rochester.edu

Abstract: Three-dimensional classical ensembles are employed to study recollision dynamics in double ionization of atoms by 780-nm intense lasers. After recollision one electron typically remains bound to the atom for a portion of a laser cycle, during which time the nucleus strongly influences its direction of motion. The electron then escapes over a suppressed barrier, with its final momentum depending critically on the laser phase at escape. The other electron remains unbound after collision, and typically drifts out in a momentum hemisphere opposite from its motion just after the collision. Several example trajectories at intensity 0.4 PW/cm^2 with various time delays between recollision and ionization are presented.

© 2006 Optical Society of America

OCIS codes: (020.4180) Multiphoton processes (270.6620) Strong-field processes (260.3230) Ionization

References and links

1. D. N. Fittinghof, P. R. Bolton, B. Chang and K. C. Kulander, "Observation of nonsequential double ionization of helium with optical tunneling," *Phys. Rev. Lett.* **69**, 2642 (1992).
2. B. Walker, B. Sheehy, L. F. DiMauro, P. Agostini, K. J. Schafer and K. C. Kulander, "Precision measurement of strong field double ionization of helium," *Phys. Rev. Lett.* **73**, 1227 (1994).
3. R. Dörner, Th. Weber, M. Weckenbrock, A. Staudte, M. Hattass, R. Moshhammer, J. Ulrich, and H. Schmidt-Böcking, "Multiple Ionization in Strong Laser Fields," *Advances in Atomic, Molecular, and Optical Physics* **48**, 1-35 (2002).
4. A. Becker and F.H.M. Faisal, "Intense-field many-body S-matrix theory," *J. Phys. B* **38**, R1 -R56 (2005).
5. A. Becker, R. Dörner, and R. Moshhammer, "Multiple fragmentation of atoms in femtosecond laser pulses," *J. Phys. B* **38**, S753-S772 (2005).
6. P. B. Corkum, "Plasma perspective on strong field multiphoton ionization," *Phys. Rev. Lett.* **71**, 1994 (1993).
7. K.C. Kulander, K. J. Schafer and J.L. Krause, in *Super Intense Laser-Atom Physics*, B. Piraux, A. L'Huillier and K. Rzazewski, Eds. (Plenum, New York, 1995), p. 95.
8. K. C. Kulander, J. Cooper, and K. J. Schafer, "Laser-assisted inelastic rescattering during above-threshold ionization," *Phys. Rev. A* **51**, 561-568 (1995).
9. G.L. Yudin and M. Y. Ivanov, "Physics of correlated double ionization of atoms in intense laser fields: Quasistatic tunneling limit," *Phys. Rev. A* **63**, 033404 (2001).
10. Hugo W. van der Hart, "Sequential versus non-sequential double ionization in strong laser fields," *J. Phys. B* **33**, L699-L705 (2000).

11. Th. Weber, M. Weckenbrock, A. Staudte, L. Spielberger, O. Jagutzki, V. Mergel, F. Afaneh, G. Urbasch, M. Vollmer, H. Giessen, and R. Dörner, "Recoil-Ion Momentum Distributions for Single and Double Ionization of Helium in Strong Laser Fields," *Phys. Rev. Lett.* **84**, 443-446 (2000).
12. R. Moshhammer, B. Feuerstein, W. Schmitt, A. Dorn, C. D. Schröter, J. Ullrich, H. Rottke, C. Trump, M. Wittmann, G. Korn, K. Hoffmann, and W. Sandner, "Momentum Distributions of Ne^{n+} Ions Created by an Intense Ultrashort Laser Pulse," *Phys. Rev. Lett.* **84**, 447-450 (2000).
13. V.L.B. de Jesus, B. Feuerstein, K. Zrost, D. Fischer, A. Rudenko, F. Afaneh, C.D. Schröter, R. Moshhammer, and J. Ullrich, "Atomic structure dependence of nonsequential double ionization of He, Ne, and Ar in strong laser pulses," *J. Phys. B* **37**, L161-L167 (2004).
14. V.L.B. de Jesus, A. Rudenko, B. Feuerstein, K. Zrost, C.D. Schröter, R. Moshhammer, and J. Ullrich, "Reaction microscopes applied to study atomic and molecular fragmentation in intense laser fields: non-sequential double ionization of helium," *Journal of Electron Spectroscopy* **141**, 127-142 (2004).
15. L.B. Fu, J. Liu, and S.G. Chen, "Correlated electron emission in laser-induced nonsequence double ionization of helium," *Phys. Rev. A* **65**, 021406 (2002).
16. A. Becker and F.H.M. Faisal, "S-Matrix Analysis of Coincident Measurement of Two-Electron Energy Distribution for Double Ionization of He in an Intense Laser Field," *Phys. Rev. Lett.* **89**, 193003 (2002).
17. S.L. Haan, L. Breen, A. Karim, and J.H. Eberly, "Variable time lag and backward ejection in full-dimensional analysis of strong-field double ionization," *Phys. Rev. Lett.* **97**, 103008 (2006).
18. Thomas Brabec, Misha Yu. Ivanov, and Paul B. Corkum, "Coulomb focusing in intense field atomic processes," *Phys. Rev. A* **54** R2551-4 (1996).
19. Phay J. Ho, R. Panfili, S.L. Haan, and J.H. Eberly, "Nonsequential Double Ionization as a Completely Classical Photoelectric Effect," *Phys. Rev. Lett.* **94**, 093002 (2005).
20. R. Panfili, S.L. Haan, and J.H. Eberly, "Dynamics of classical slow-down collisions in non-sequential double ionization," *Phys. Rev. Lett.* **89**, 113001 (2002).
21. Pierre Agostini and Louis F. DeMauro, "The physics of attosecond light pulses," *Rep. Prog. Phys.* **67**, 813-855 (2004).
22. G.G. Paulus, W. Becker, W. Nicklich, and H. Walther, "Rescattering effects in above-threshold ionization: a classical model," *J. Phys. B* **27**, L703-L708 (1994).

1. Introduction

It is now generally accepted that non-sequential double ionization (NSDI) of atoms [1]- [5] occurs through recollision [6, 7], a process in which one electron first departs the atom but then is impelled back to the atomic core by oscillations in the laser field. The ensuing recollision may directly ionize the other electron or may excite the second electron to a state from which it can subsequently laser ionize [8, 9]. Questions then arise regarding the lifetime of the excited state [10] and whether the final momentum distributions [11, 12] of the electrons can serve as signatures of various processes. For example, experiments in helium have shown that doubly ionized electron pairs can emerge in either the same or in opposite momentum hemispheres relative to the laser polarization axis [13, 14], while theoretical treatments (for example [15] and [16]) indicate that direct recollision ionization should lead to same-hemisphere electrons. Of course, collisional excitation with subsequent ionization occurring significantly later in the pulse can be expected to lead to uncorrelated momenta and thus some opposite-hemisphere electrons.

In a recent Letter [17] we introduced the use of three-dimensional classical ensembles for studying double ionization. We showed that for laser wavelength 780 nm and intensities 0.4 to 1.2 PW/cm² there is typically a time delay of a portion of a laser cycle between recollision and double ionization. This brief time delay allows for a middle ground between direct recollision ionization and recollision excitation with subsequent uncorrelated ionization. We found in particular that to first approximation same-hemisphere or opposite-hemisphere electrons could result depending on whether the final ionization occurred before or after the field maximum that followed the recollision.

In the present work we extend our classical ensemble analysis. In Section 2 we review and expand on the ensemble results of Ref. [17], paying particular attention to laser intensity 0.4 PW/cm². Then in section 3 we examine individual trajectories that lead to same-hemisphere

and opposite-hemisphere ejections. We look at trajectories that have various time delays and examine the dynamics of the double-ionization process.

Each of our ensembles contains 400,000 model atoms. The ensemble was populated starting from a Gaussian spatial distribution in each of x , y , and z , filtered to keep only classically allowed positions for the helium ground-state energy of -2.9035 au. The available kinetic energy was distributed between the electrons using a random number in momentum space. Each electron was given radial velocity only, with sign randomly selected. Then, and very importantly, the system was allowed to evolve for a time equivalent to one laser cycle (about 100 au) with no laser field. This time period was more than sufficient to ensure stable position and momentum distributions. During this evolution the electrons exchange energy and angular momentum, but the net values of these quantities remain fixed at -2.9035 au and zero respectively. We have considered several starting ensembles, including one that is based on the quantum ground state, and found that details of the starting configuration matter very little, as long as we begin with spherically symmetric probability distributions for each electron and only radial velocities. To prevent self-ionization, we shield the electron-nuclear interaction [18]. The full Hamiltonian of our system is

$$H = \frac{p_1^2}{2} + \frac{p_2^2}{2} - \frac{2}{\sqrt{r_1^2 + a^2}} - \frac{2}{\sqrt{r_2^2 + a^2}} + \frac{1}{\sqrt{(\vec{r}_1 - \vec{r}_2)^2 + b^2}} + (z_1 + z_2)E_0 f(t) \sin(\omega t) \quad (1)$$

where $a = 0.825$ au, $b = 0.05$ au, and where $f(t)$ is a pulse shape parameter (we use atomic units throughout this paper). We use a trapezoidal pulse with two-cycle turn on, six cycles at full strength, and two-cycle turn off. The linearly ramped laser turn off does not alter the drift velocity of a free electron. Our laser frequency is 780 nm.

2. Ensemble Results

In Fig. 1 we present density plots of final momentum components parallel to the laser-polarization (z) axis for doubly ionized electron pairs produced at laser intensity 0.4 PW/cm^2 . As for Fig. 2 of Ref. [17], which considered intensity 0.6 PW/cm^2 , we have back analyzed each trajectory and found the times of recollision and ionization. We define the time of recollision to be the time of closest approach of the two electrons after departure of one electron from the core, and we define an electron to be ionized if its energy (calculated as kinetic plus the nuclear and e-e potential energies) is greater than zero or if it is outside the nuclear well (specifically, $|z| > 2.2$ with the z component of the laser force plus nuclear force away from the nucleus). We have also assigned signs for each final p_z so that positive coordinates indicate final drift in the same momentum hemisphere relative to the z axis as the returning electron's momentum just before recollision; we will refer to this situation as having an electron emerge in the "direction" of the recollision. Figure 1 differs from Fig. 2 of Ref. [17] in two ways other than laser intensity—in the present work we define the returning electron to be electron two, and we present non-overlapping time intervals.

The first plot in Fig. 1 shows that for ionizing trajectories with small delay times between recollision and ionization, the electrons in each pair emerge in the same momentum hemisphere (i.e., with the same sign for p_z), but opposite from the recollision. With increasing delay times, the plots show increasing numbers of trajectories in quadrants two and four, which indicate opposite-hemisphere electron pairs. Delay times of greater than 0.5 cycle lead to basically uncorrelated emissions, although the small number of trajectories in the first quadrant indicate that it is unlikely for both electrons to emerge in the direction of recollision. The asymmetry about the line $p_{2z} = p_{1z}$ indicates that on average the recolliding electron has less final energy than the struck electron. The boxes in each plot show the values of $(4U_p)^{1/2}$, the maximum

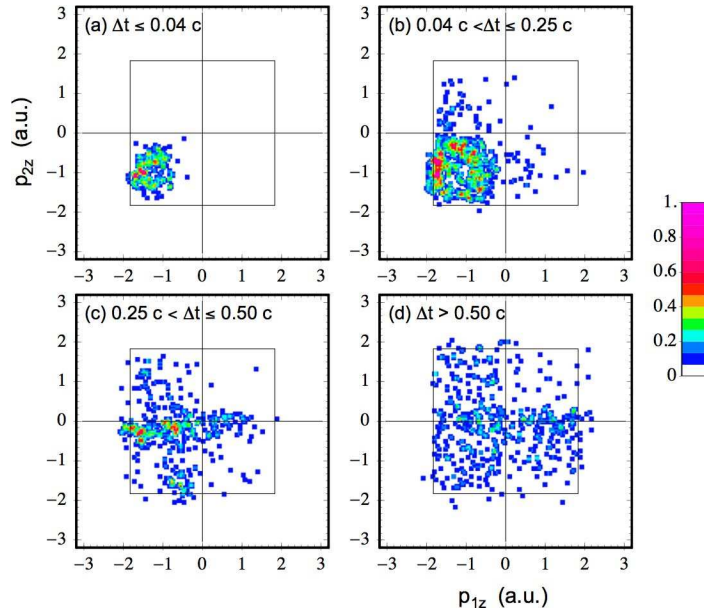


Fig. 1. Scatter plots of final momentum components along the laser polarization axis for laser intensity 4×10^{14} W/cm² and for the indicated time delay intervals between recollision and double ionization. For each trajectory, p_{2z} denotes final z-component of the momentum of the recolliding electron, and p_{1z} the struck electron. The signs of the final momenta are defined so that all recollision events occur with the recolliding electron having $p_{2z} > 0$. The boxes show $(4U_p)^{1/2}$, with $U_p=0.838$ au. For time delays less than 0.25 cycle, most electrons emerge in the momentum hemisphere opposite from recollision, so $p_z < 0$ in the plot.

drift momentum for a classical electron that starts from rest and is subjected only to an oscillating electric field. Here U_p denotes the ponderomotive energy, $E_0^2/(4\omega^2)$. The final momenta generally do not exceed $(4U_p)^{1/2}$, although the plots do show some exceptions, especially for the struck electron. Plot (c) also shows some clustering along the negative p_{1z} axis, indicating numerous trajectories for which the recolliding electron (electron 2) drifts slowly outward opposite from the collision.

As a first step toward explaining the results of Fig. 1, we show in Fig. 2 the laser phases for recollision and double ionization for laser intensity 0.4 PW/cm². The red and green bands respectively represent the same- and opposite-hemisphere trajectories that have time lag less than a chosen upper bound, with blue representing all the other doubly ionizing trajectories. In the first row, the upper bound on the time delay is 1/25 cycle, in the second row 1/4 cycle, and the third row 1/2 cycle. The fourth row classifies all trajectories as same or opposite hemisphere regardless of time delay. The most conspicuous result of Fig. 2 is the phase difference between recollision and ionization. The recollision times of doubly ionizing trajectories peak shortly before the zeroes of the laser field, when in the Corkum model [6, 7] the recolliding electrons can be expected to have maximum energy. Double ionizations peak shortly before the maxima of the laser field, when the potential energy barrier that confines the inner electron is maximally suppressed and when recollisions occur the least. We also note that ionization leading to the opposite-hemisphere trajectories peaks close to or just after the field maximum, especially for delay times less than 0.50 cycle. Thus Fig. 2 illustrates for intensity 0.4 PW/cm² the conclusion of Ref. [17] that a time lag between recollision and double ionization can be associated with

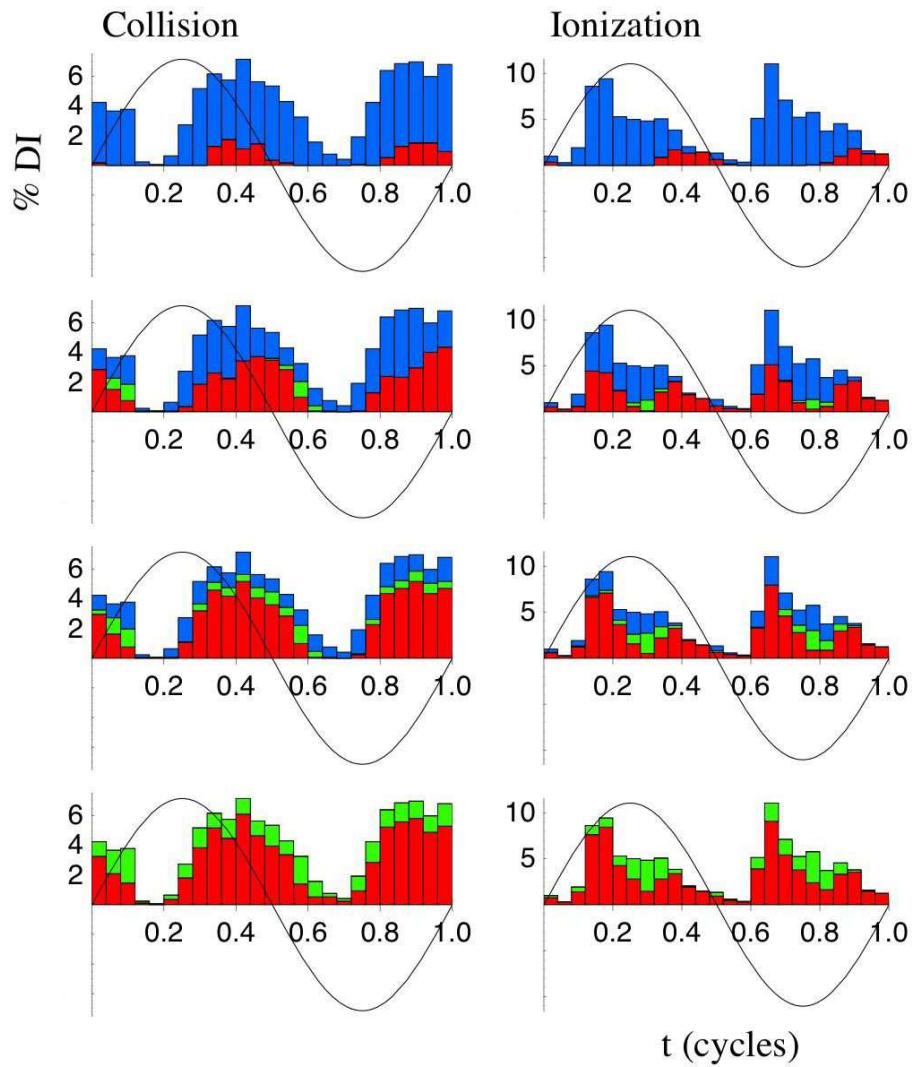


Fig. 2. Percent of doubly ionizing trajectories vs. laser phase for recollision (left column) and double ionization (right column) for laser intensity 4×10^{14} W/cm². The red and green respectively show the same-hemisphere and opposite-hemisphere trajectories for various maximum time lags, with blue giving all remaining DI trajectories. The top three rows show time delays of less than 1/25 cycle, 1/4 cycle, and 1/2 cycle respectively. The fourth row classifies all trajectories as same- or opposite-hemisphere regardless of time delay. The phase difference between recollision and double ionization is clearly evident.

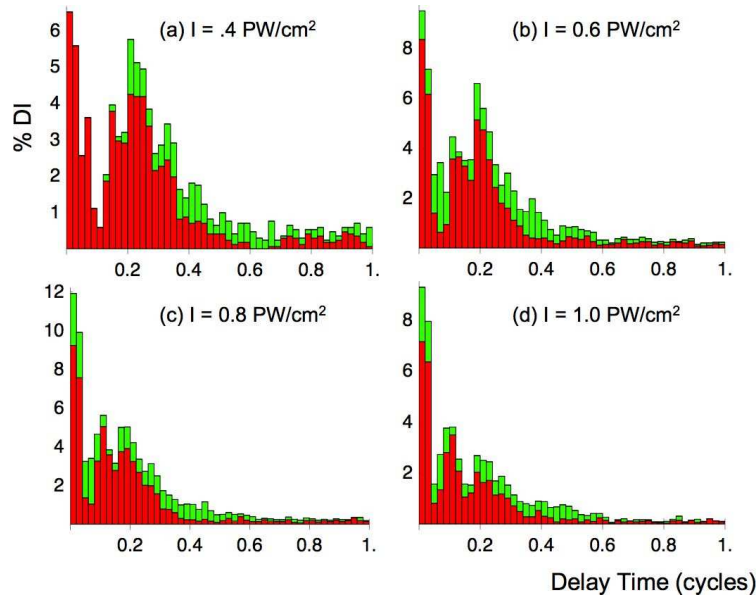


Fig. 3. Distribution of time delays for four different laser intensities. Red and green indicate same-hemisphere and opposite-hemisphere trajectories, respectively. Plots only extend to a delay time of 1 cycle, but there are scattered delay times up to 6.9 cycles. The percent of DI trajectories with delay times of one cycle or less are 86%, 88%, 90%, and 89%, for the respective laser intensities. Total yields for the four intensities were 1721, 3503, 4320, and 4927 trajectories of 400,000.

the opposite-hemisphere trajectories that are observed in experiment [13, 14].

In Fig. 3 we present the distribution of time delays for laser intensities 0.4, 0.6, 0.8 and 1.0 PW/cm^2 . Each plot shows a cluster of trajectories for very small time delays, corresponding with direct or nearly direct recollision ionization. For intensity $0.4 \text{ PW}/\text{cm}^2$ electrons can be expected to recollide with energy up to about $3.2U_p = 2.7 \text{ au}$. The ground state energy of He^+ is of course -2 au , and the maximum depth of our classical well is $-2/.825 \text{ au} = -2.42 \text{ au}$. Thus one might expect direct recollision ionization to dominate the double ionization. However, each plot in Fig. 3 shows a second peak at delay times of about 0.2 cycle. Median delay times are 0.26, 0.20, 0.16, and 0.16 cycles for (a)-(d) respectively.

3. Trajectory Analysis

In this section we show representative two-electron trajectories. We cannot show all the variations among the trajectories, but have selected trajectories with key features for understanding the classical DI process. The trajectories are for laser intensity $I = 0.4 \text{ PW}/\text{cm}^2$. The electrons are depicted in blue and red, and the stationary nucleus as a small black dot. The arrows show the laser force.

We begin by considering a two-electron trajectory that exhibits direct recollision ionization. The still image on the left side of Fig. 4 shows $t=3.90$ cycles, shortly after the recollision and as the two ionized electrons exit the frame in the direction of the laser force. The movie begins at $t=2.50$ cycles. One electron is ionized when the field is strong, then returns for a recollision at $t=3.42$ cycles. The recollision directly ionizes the second electron. The direction of the laser force changes after $t=3.5$ cycles, causing the electrons to change direction after the recollision. The drift velocity of an electron in one dimension subjected only to an oscillating electric field

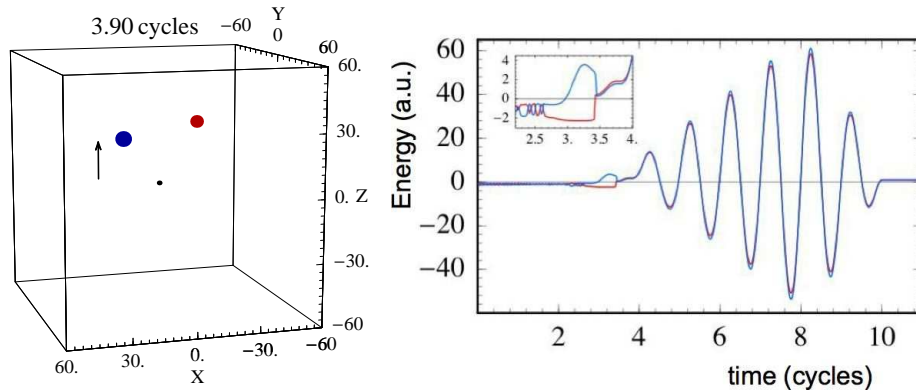


Fig. 4. On the left is a movie (64 kB) of one two-electron trajectory that exhibits direct recollision ionization for laser intensity $I = 0.4 \text{ PW/cm}^2$. There is a change in direction of the electrons after recollision. The still shows time 3.90 c with both electrons traveling outward after ionization. On the right is an energy vs time plot for the two electrons. The energy transfer at recollision is clearly visible in the inset.

is $v_0 \pm (4U_p)^{1/2}$, where v_0 is the electron velocity at the field zero and where the positive or negative sign is chosen depending on whether the laser force after the field zero is parallel or antiparallel to the direction of motion. In this case the laser causes a change in direction of motion and we need the negative sign. The resulting cancellation ensures that each electron has final momentum less than $(4U_p)^{1/2}$, and having $v_0 < (4U_p)^{1/2}$ leads to drift opposite from the direction of recollision.

On the right side of Fig. 4 we plot energy vs. time for each electron. This plot is similar to ones we showed in Ref. [19]. The various stages of double ionization are clearly visible—the initial jostling of the two bound electrons, the first ionization, the recollision, the final ionization, and the final oscillation of the electrons in the laser field until the laser is fully turned off. Immediately after the collision, both electrons have energy greater than zero, as shown in the inset. We have included the $zE_0f(t)\sin(\omega t)$ interaction energy, and thus after ionization the energy is dominated by the electrons' potential energies. The electrons are on the same side of the atom and oscillate in phase.

Figures 5 and 6 present a trajectory that has time delay of 0.18 cycle between recollision and double ionization. This time delay is clearly visible just after $t=8 \text{ c}$ in Fig. 5, with one electron having energy less than zero after the collision. The movie shows that the struck electron is pushed to the side (the negative x direction) by the recollision. It travels part way around the nucleus before escaping into the negative- z hemisphere as the laser field grows stronger. The recolliding electron, which still has positive energy after the recollision, overshoots the core but the laser force subsequently propels it back in the opposite direction, so that the two electrons emerge in the same momentum hemisphere. The struck electron finishes with considerably more energy than the recolliding electron.

On the right side of Fig. 6 we superpose the z -part of the motion with color-coded effective-potential-energy curves for the electrons. This plot format generalizes effective-energy plots that we introduced in 1-d studies [20]. The curves are drawn as functions of z , but have parametric dependence on the x and y coordinates of the electrons, for example

$$V_{eff1}(z) = -\frac{2}{\sqrt{x_1^2 + y_1^2 + z^2 + a^2}} + \frac{1}{\sqrt{(x_1 - x_2)^2 + (y_1 - y_2)^2 + (z - z_2)^2 + b^2}}$$

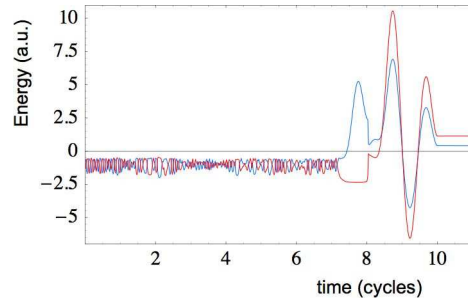


Fig. 5. Energy plot for a double ionization that has delay time 0.18 cycle between recollision and final ionization.

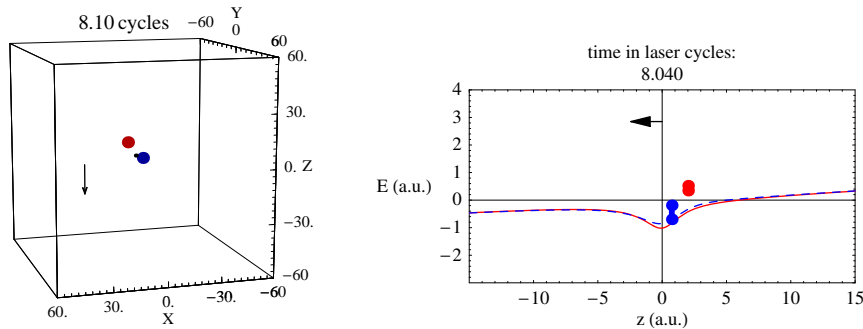


Fig. 6. Movies (72 and 244 kB) of the trajectory of Fig. 5. The right plot shows the z-part of the motion, with effective potential energy plots for each electron. The curves have a parametric dependence on the x and y values. The still images show times shortly after recollision when the struck (blue-coded) electron still has energy less than zero.

$$+zE_0f(t)\sin(\omega t) \quad (2)$$

The parametric dependence on the x and y coordinates is very clear in the movie. For example, the depth of the well for each electron depends on the value of $\rho_i = (x_i^2 + y_i^2)^{1/2}$, being deepest when $\rho_i = 0$ and flattening out as ρ_i increases. Also, if the electrons have similar x and y values, so that changing just the variable z for either electron could lead to near collision, then the effective potential energy curves show repulsive barriers beneath each electron. The vertical separation of each dot from the correspondingly colored potential-energy curve is determined by the electron's kinetic energy. In frames in which two dots and a connecting bar are visible for an electron, the top dot gives the electron's full energy while the lower dot excludes portions of the kinetic energy from motion perpendicular to the laser polarization.

In the movie, the recollision occurs from left to right. The collision pushes the struck electron toward positive z, but it "bounces" off the potential energy barrier and returns back toward negative z. Its brief motion in the x direction that was apparent in the left-hand-movie is evidenced here by the brief appearance of the vertical bar. The electron reaches the negative z side of the nucleus as the laser field is growing stronger and suppressing the nuclear barrier. Even though the electron has energy less than zero, it has more than enough energy to escape over this suppressed barrier. This trajectory illustrates how there can be a recollision that does not ionize the struck electron immediately but nonetheless leads to correlated electron emission. In examining the movie it's important to remember that the effective potential energies are defined so that the z component of the force is minus the derivative of the potential and for each electron includes

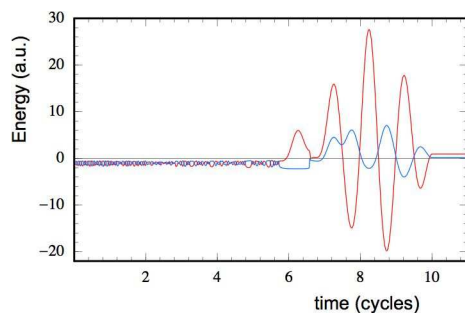


Fig. 7. Energy vs. time for a trajectory that features opposite-hemisphere electrons. The second ionization occurs *after* the field maximum at 6.75 c.

the *full* electron-electron repulsion. Thus the sum of the effective individual energies counts the e-e repulsion twice and exceeds the total energy. This explains why the plots may seem on first inspection to violate energy conservation when the electrons are very close together.

Figures 7 and 8 illustrate a trajectory that leads to opposite-hemisphere electrons. The recollision occurs at 6.588 cycles, and final ionization at 6.79 cycles—after the field maximum. The late-ionizing electron begins to follow the other electron out in the positive z direction, but after the laser field changes sign the electron is propelled back and drifts out in the opposite, $-z$, direction. We noted above the well-known result that the drift velocity of an electron exposed only to an oscillating electric field is $v_0 \pm (4U_p)^{1/2}$, where v_0 is the electron velocity at the field zero. The drift velocity also equals the velocity of the electron at the field maximum. Thus an electron that ionizes before the field maximum will have velocity in the direction of its escape at the time of the maximum and can be expected to continue out in that direction, unless pulled back by the nucleus. However, an electron that escapes after the field maximum can be expected to drift out in the hemisphere opposite from its original escape. Such an electron can also scatter off the bare nucleus and be a source of high harmonics [21]. It could also backscatter off the nucleus and thus obtain higher energy [22]. Unfortunately, we cannot expect our model to predict those high-energy backscattered electrons, since we shield the nuclear force.

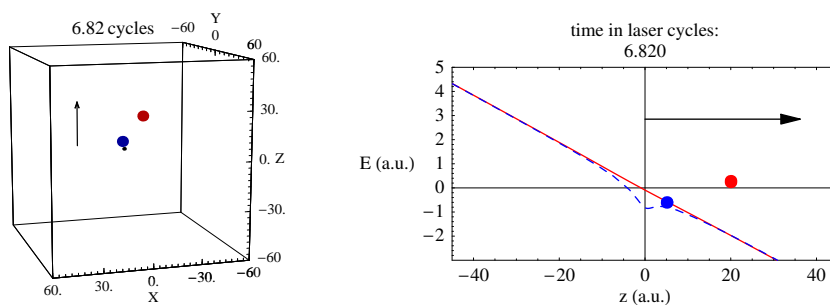


Fig. 8. Trajectory and effective energy movies (132 and 964 kB) for the trajectory of Fig. 7. The struck electron ionizes after the field maximum and drifts out opposite from its initial ionization. Still images are shortly after ionization, which by our definition occurs at 6.79 c.

The time delay for the trajectory of Fig. 8 is 0.20 cycle, and the struck electron does an extra oscillation in the nuclear well before escaping. We emphasize that the specific reason that the electrons emerge in opposite hemispheres is the laser phase at the time of the final ionization,

and not the size of the time delay or the number of oscillations in the nuclear well between recollision and final ionization. We also note that the condition of emission after the field zero to obtain opposite hemisphere electrons is just a first approximation. The histogram of ionization times in Fig. 2 shows that some ionizations for opposite-hemisphere emissions occur slightly before the field maximum. An examination of those reveals that the coulombic attraction of the nucleus pulls the electron back, so that it can drift out in the opposite hemisphere.

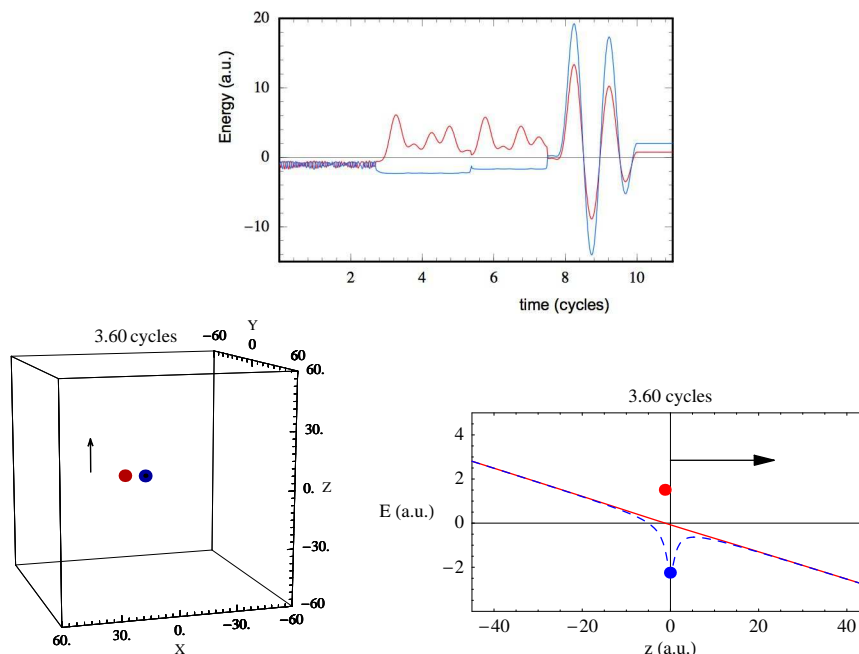


Fig. 9. Energy and trajectory plots for a trajectory that illustrates other characteristics—a miss, coulomb focusing, multiple recollision, and electron exchange. Movies are 240 and 792 kB.

The above trajectories were chosen to illustrate important ideas in the double ionization recollision process. There are other characteristics that appear in individual trajectories. Rather than introduce those one by one, we show a trajectory that combines several additional features. In Fig. 9 the returning electron crosses the $z=0$ plane several times without striking the nucleus before coulomb focusing [9, 18] pulls it in for recollision at $t=5.35$ cycles. For this particular trajectory, the first recollision excites the inner electron but does not ionize it. A second recollision leads to ionization. In the second collision, there is electron exchange, so that the recolliding electron has less energy than the struck electron after the collision. We have found that electron exchange occurs in approximately 30% of the trajectories at this intensity. In the trajectory of Fig. 9 the electrons emerge nearly together and the exchange is relatively unimportant. In other trajectories however there is a clear electron “swap,” with the struck electron becoming unbound and overshooting the nucleus, while the recolliding electron has the nucleus-induced direction change discussed above.

4. Summary

In this work we have built on Ref. [17], in which we introduced the use of fully 3-d classical ensembles for studying non-sequential double ionization. In that work we showed that for laser wavelength 780 nm and intensities 0.2 to 1.2 PW/cm², direct recollision ionization accounts

for less than 15% of the doubly ionizing trajectories of our model, regardless of whether the returning electron has sufficient energy that both electrons could be free. We have seen that when direct recollision ionization does occur, it typically leads to an electron pair that travel into the same momentum hemisphere. After direct recollision ionization there is a laser-induced direction change in the motion of the electrons relative to the laser polarization axis, and because of this direction change the electrons have drift energy less than $2U_p$ and drift momentum less than $(4U_p)^{1/2}$.

We have found that recollisions occur most often just before the laser field goes through zero and least often just before a field maximum, whereas final ionizations peak just before the field maximum. Thus there is usually a time delay between recollision and ionization, during which one of the electrons remains bound. This electron usually ionizes the first time the laser field peaks after recollision, and the projection of its motion onto the laser-polarization axis is opposite in direction from the recollision. The mechanism, which can be described as “recollision, bounce, and escape,” proceeds basically as follows: If the recollision pushes the electron in say the +z direction, where the z axis is the laser polarization axis, the nucleus stops that motion and pulls the electron back in the -z direction (the changing laser field can of course contribute to this direction change); a more three-dimensional description is that the still-bound electron “swings around behind the nucleus.” Then if the timing is such that the electron comes back to the -z side of the nucleus and moving in the -z direction as the laser suppresses the confining well, the electron can escape over the barrier. The time of the ionization plays a fundamental role in determining the final momentum distributions of the electron pairs. To first approximation, if the final ionization occurs before the laser field peaks, the electrons will travel out from the atom in the same hemisphere, opposite from the recollision. However, if the second electron ionizes after the laser field peaks, then to first approximation, electrons will travel out from the atom in opposite momentum hemispheres. We thus find that we don’t need direct recollision ionization to obtain correlated electrons, but also that we don’t need long time delays of a half cycle or more to obtain opposite-hemisphere electrons.

In Fig. 1 we found that the recolliding electron is often the slower of the two electrons after the pulse. This result is easily explained by noting that the recolliding electron is usually unbound after the recollision and will experience a laser-induced direction change in its motion. Thus its energy is limited to $2U_p$, the maximum drift energy for an electron that starts from rest in an oscillating laser field. The other electron has a nucleus-induced direction change, as described in the previous paragraph, and is not necessarily limited to energy $2U_p$. We will examine its energy characteristics elsewhere.

In about 30% of the doubly ionizing trajectories there is an electron swap at recollision, so that the returning electron has less energy than the struck electron. This swap explains the many exceptions to the post-collision behavior of the struck vs. recolliding electron discussed in the preceding paragraph.

The basic sequence of events in the trajectories is really very similar to what we found in studying the one-dimensional quantum model[20]. The primary difference is that in the one-dimensional model the timing for collision, bounce, and escape over a suppressed barrier worked best for slowdown collisions, i.e., for recollisions that occurred after the laser minimum. In three dimensions a greater range of laser phases at recollision can be effective.

It may be surprising to some readers that our model shows so little direct recollision ionization. We make two comments in this regard. First, not all collisions are efficient for transferring energy. In our ensemble, the recolliding electron returns at a variety of impact parameters and encounters the inner electron at various points in its oscillation in the nuclear well. Second, we note that some collisions are *too* efficient in transferring energy, so that the struck electron is ionized and the returning electron briefly recaptured. It is only in the minority of cases that

there is a collision such as we show in the trajectory of Fig. 4 that leaves both electrons with positive energy.

Acknowledgements

This material is based upon work supported by the National Science Foundation under Grant No. PHY-0355035 to Calvin College and by DOE Grant DE-FG02-05ER15713 to the University of Rochester.